

Article

# Superscattering and Directive Antennas via Mode Superposition in Subwavelength Core-Shell Meta-Atoms

Alexander W. Powell , Michal Mrnka, Alastair P. Hibbins and J. Roy Sambles

Department of Physics and Astronomy, University of Exeter, Exeter EX4 4QL, UK; m.mrnka@exeter.ac.uk (M.M.); A.P.Hibbins@exeter.ac.uk (A.P.H.); j.r.sambles@exeter.ac.uk (J.R.S.)

\* Correspondence: a.w.powell@exeter.ac.uk; Tel.: +44-13-9272-4187

**Abstract:** Designing a subwavelength structure with multiple degenerate resonances at the same frequency can vastly enhance its interaction with electromagnetic radiation, as well as define its directivity. In this work we demonstrate that such mode superposition or ‘stacking’ can be readily achieved through the careful structuring of a high-permittivity spherical shell, with either a metallic or a low permittivity dielectric (air) core. We examine the behaviour of these structures both as scatterers of plane wave radiation and as directive antennas. In the case where the core is metallic this leads to a superposition of the magnetic and electric modes of the same order, causing suppression of backscattering and unidirectional antenna emission. For an air core, an electric mode can superimpose with the next-highest order magnetic mode, the backscattered power is maximized and antenna emission is bidirectional. This is shown experimentally at microwave frequencies by observing the backscattering of core-shell spheres and we propose two antenna designs demonstrating different emission patterns defined by the superposition of multiple modes.

**Keywords:** superscattering; subwavelength; dielectric; antenna; resonant; microwave; radar cross section



**Citation:** Powell, A.W.; Mrnka, M.; Hibbins, A.P.; Sambles, J.R. Superscattering and Directive Antennas via Mode Superposition in Subwavelength Core-Shell Meta-Atoms. *Photonics* **2022**, *9*, 6. <https://doi.org/10.3390/photronics9010006>

Received: 17 November 2021

Accepted: 17 December 2021

Published: 22 December 2021

**Publisher’s Note:** MDPI stays neutral with regard to jurisdictional claims in published maps and institutional affiliations.



**Copyright:** © 2021 by the authors. Licensee MDPI, Basel, Switzerland. This article is an open access article distributed under the terms and conditions of the Creative Commons Attribution (CC BY) license (<https://creativecommons.org/licenses/by/4.0/>).

## 1. Introduction

The resonant modes of a subwavelength structure define its interaction with electromagnetic radiation and are fundamental to the operation of many types of antennas, sensors, and metamaterials. Any given resonance will have an associated charge, current or displacement current in a given structure, which corresponds to a specific farfield radiation pattern. In many conventional structures, the fundamental natural resonances are separated in frequency and do not spectrally overlap significantly. In recent years however there has been a growing interest in the use of tailored systems where two or more resonant modes can be superimposed or ‘stacked’—made to share a resonant frequency, leading to enhanced interaction with electromagnetic radiation and improved directivity in the farfield [1–15]. The combination of the lowest order (dipole) modes—a Huygens source, has been widely explored [3,4,11–15], but the stacking of higher order modes has received less attention. Ruan and Fan [5] proposed a multilayered rod structure which could combine several electric resonances to achieve mode stacking. Liu et al. [8] later proposed using a metal-dielectric core-shell spherical geometry to superimpose both electric and magnetic modes. However, this proved difficult to replicate experimentally, and the first demonstrations of superscattering of a plane wave via the superposition of higher order resonances have only been published recently by Qian et al. [1], and the authors [16].

Mode stacking has enabled significant progress in controlling the power and directionality of radiation scattered by resonant particles when illuminated by a plane wave, which is key for technologies from light trapping in solar cells [17,18] to radar detection [19]. The spectral overlap of two or more modes in a variety of geometries has produced powerful scattering, that surpasses the theoretical single channel limit [20] in both the microwave [1,2,15] and optical regimes [14,21] as well as producing directional emission

and suppressed backscatter. The opposite case, where backscattered power is maximized, has also been posited theoretically by Liberal et al. [22] and Nagarhi et al. [23] who demonstrated that overlapping modes with equivalent phase of radiation in the reverse direction leads to a maximization of backscattered power, which has been recently experimentally verified by the authors [16].

A second key area where mode stacking is producing important results is the field of dielectric resonator antennas (DRAs). High-permittivity ceramics have been structured to overlap pairs of modes and produce unilateral emission [24–26] as well as multiple modes simultaneously to produce highly directional emission [27–29], and water-based antennas have also shown the capacity to act as an easily fabricable Huygens source [30]. In all cases however the choice of mode combinations is somewhat limited and does not reflect the variety of emission patterns that can be achieved by structuring the resonator in order to overlap different choices of modes. For many structures it is very difficult to simultaneously excite different mode orders with a single feed—Boyuan et al. [24] utilize symmetry breaking to create an electric dipole-like resonance from the magnetic dipole, which is effective, but would be difficult to replicate for higher order modes. Jacobsen et al. [30] use water-filled structures to create resonances, which would not easily support the high Q-factors of higher order resonances due to losses in the water. A structure where multiple mode orders can be manipulated and stacked to control the directionality would be hugely beneficial for DRA research.

In this study we show the versatility of a simple, high symmetry geometry—a two layer (core-shell) sphere for utilizing mode stacking to control microwave emission when resonances are driven either by a plane wave or by an antenna feed. We draw parallels between the two cases to demonstrate the applicability of the physics to a variety of fields. In terms of scattering, we show how the radius of different core-shells structures can cause different combinations of modes to overlap spectrally, either suppressing or enhancing the backward scatter. We experimentally demonstrate this using a metallic core to combine the electric and magnetic dipoles in order to reduce backward scatter, and an air core to combine the electric dipole and magnetic quadrupole to enhance it. Finally, we show that these same geometries can also be used to create unidirectional and bidirectional dielectric resonator antennas and we propose two designs to demonstrate this.

## 2. Materials and Methods

All scattering simulations were conducted in Comsol Multiphysics using the RF module. A 12.5 mm radius sphere with a permittivity  $\epsilon = 10.5$ , loss tangent,  $\delta = 0.001$  is modelled in empty space surrounded by a perfectly matched layer (PML) shell. Samples are excited via an incident plane wave of frequencies between 3–9 GHz. Either an air-filled spherical cavity or a spherical metal ball is defined at the centre of the sphere, and its monostatic radar cross section (RCS) and scattering cross section are calculated in the far field as the radius of this core is changed from 0–6.5 mm.

Experimental RCS measurements were conducted using a quasi-monostatic setup in an anechoic chamber. Samples were three 12.5 mm radius spheres (each milled as two hemispheres) from premix 1050 (permittivity in the low GHz regime of  $\epsilon = 10.5$ , loss tangent,  $\delta = 0.001$ ) [31]. A 5 mm radius cavity was milled at the centre of one sphere to maximize backscatter while a 4 mm radius cavity coated with conducting silver paint (acting as a metallic core) was milled in a second to minimize backscatter. The samples are shown in Figure 1a, and were mounted on a fiberglass pole topped with Rohacell 31HF foam, chosen for its extremely low relative permittivity ( $\epsilon = 1.04$ ) and we make the assumption that the impact of this substrate on the scattering behaviour of the spheres is negligible. Microwave radiation was provided via an Anritsu MS46122B VNA and a DP240-AB Dual-polarisation horn antenna from Flann Microwave located 3 m from the sample, a distance at which the curvature of incident radiation across the sample will be negligible and the radiation can be described as a plane wave in the region of the sample. The RCS is measured quasi-monostatically using a second antenna, located adjacent to the

emitting antenna and separated by a metallic plate to minimize crosstalk between antennas. All measurements are calibrated using a 12 mm radius brass sphere and a time gating function was utilized to minimize unwanted reflections.

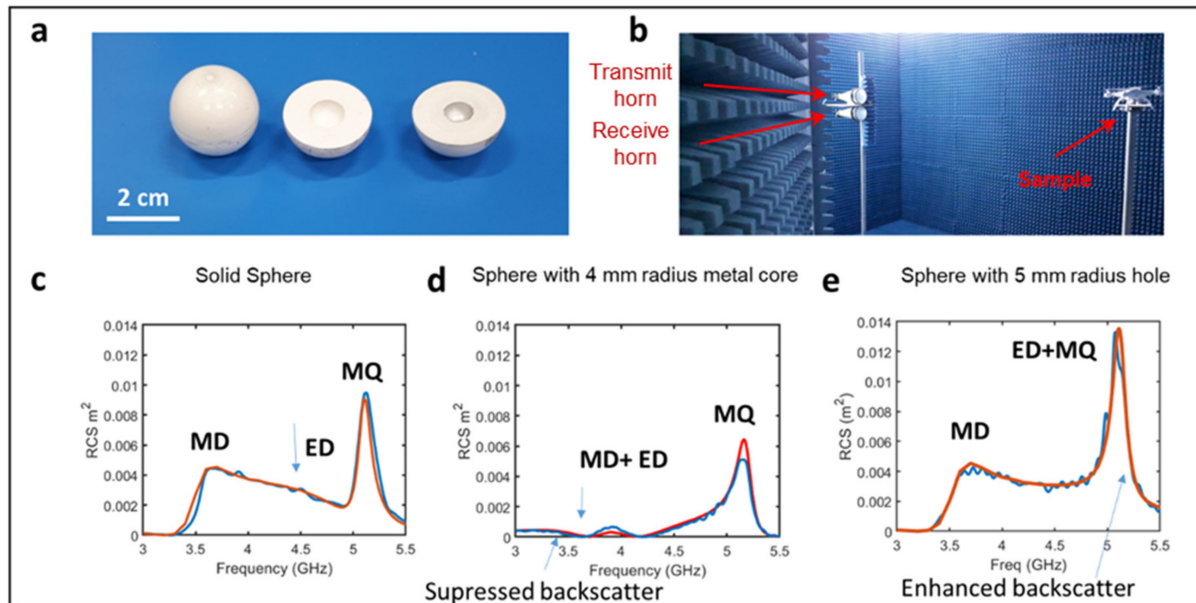


**Figure 1.** Experimental demonstration of suppression and enhancement of backscatter through mode stacking. (a) Spherical samples milled as two hemispheres from premix 1050. From left to right—solid, 5 mm radius hole and 4 mm radius metallic core. (b) The anechoic chamber used to take experimental data set up for quasi-monostatic RCS measurements. Experimental (blue) and simulated (red) RCS of (c) a solid sphere, (d) a sphere with a 4 mm metal core and (e) a sphere with a 5 mm radius hole.

Antenna simulations were conducted using a commercial, finite element method based software tool Ansys HFSS (Canonsburg, PA, USA). A hemisphere of the dielectric described above is modelled with its flat face flush with a perfect electric conductor (PEC), which serves as a ground plane. The PEC ground plane assumes infinitely small thickness and infinitely large lateral extent. The edge effects are thus not part of the simulation. All the metallic parts are considered PEC and the only losses included in the model are related to the dielectric hemispheres.

The feed for solid hemisphere antennas consists of a 4.8 mm long, 1.8 mm diameter linear current probe. The probe is fed by a short section of a PTFE-filled coaxial cable with a diameter of 4.1 mm. The coaxial feed is excited with a fundamental TEM wave with characteristic impedance of 50 Ω. For antennas with metallic cores, the excitation consists of a 6 mm long, 1.8 mm diameter linear probe connected to a PTFE filled coaxial cable with 50 Ω impedance. The probe position and the metal core radius are swept in order to tune the excitation of different modes, and the far-field radiation pattern and S11 parameter as a function of frequency are calculated.

### 3. Results

The principle of mode stacking is laid out in Figure 2. Through examining the far-field radiation pattern for each fundamental (Mie) resonance of a dielectric sphere, it can be seen that forward and reverse scattered light will possess a different phase depending on the scattering mode. When the far field contributions from each mode are superimposed, the scattered radiation will interfere either destructively or constructively in a given direction, leading to strong scattering in either the forward direction or in both the forward and backward directions. It is also possible to for scattering from different modes to suppress all forward scattering (second Kerker condition) but due to the symmetry conditions of

the system this is only achievable far from a resonance, and the scattering is comparatively weak [20]. Depending on the selection of the modes from which radiation interferes, the directionality of radiation can be greatly enhanced, as shown in the finite element simulation results in Figure 3.

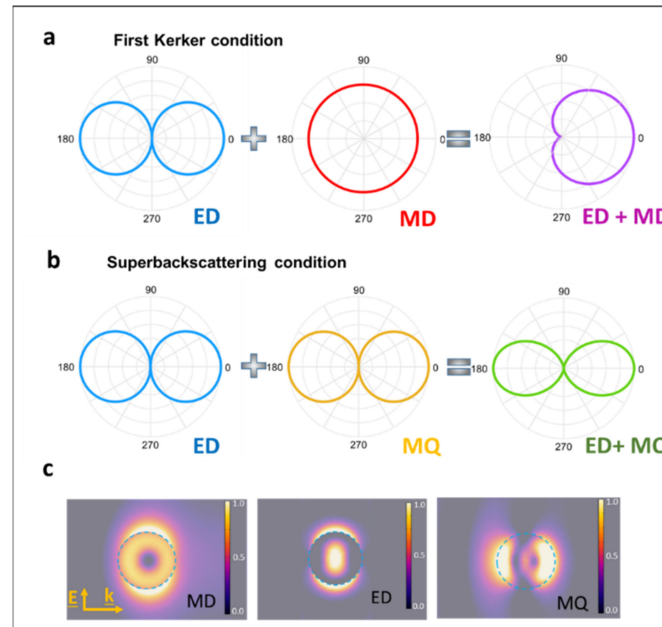


**Figure 2.** Illustrating the concept of ‘mode-stacking’ where two or more modes are superimposed spectrally and their far field patterns interfere to control the directivity of scattering (or radiation) from a dielectric sphere [16]. (a) The combination of electric and magnetic dipoles (ED + MD, first Kerker condition), leading to constructive interference in the forward direction and destructive in the reverse. (b) Shows the combination of the electric dipole and magnetic quadrupole (ED + MQ) where the emission is bidirectional and scattered power in the reverse direction is maximized (a ‘superbackscattering’ condition [22]). (c) Shows Comsol simulations of the normalised electric near-fields of these three modes. The field distributions provide clues as to how these modes can be tuned separately to achieve an overlap condition.

Obviously in order to achieve mode stacking, the multiple modes shown in Figure 2 must occur at the same frequency. As can be seen at the top of Figure 3, for a solid spherical dielectric particle ( $r_i = 0$ ) constructed of a high permittivity dielectric ( $\epsilon = 10.5$ ), the resonant modes are clearly spectrally separated. However, as Figure 2c shows, the electric near fields of the electric and magnetic modes are quite distinct, with electric modes having a significant field component at the centre of the sphere and magnetic modes being more confined to the outer rim. Therefore, as proposed theoretically by Liberal et al. [22] and Naraghi et al. [23], altering the refractive index in the central region will cause the electric modes to shift in frequency to a greater extent than the magnetic modes. This can be seen in Figure 3a, where the insertion of an air core in a high permittivity sphere leads to a blue-shifting of the electric modes until they overlap with the next-highest order magnetic modes.

The addition of a metallic core in this region can also be seen in Figure 3b to have a strong impact on both mode families. Previous reports describe mode stacking by matching the plasmon modes of a metallic core to the magnetic modes of a dielectric shell [8,32]. However at microwave frequencies the core does not support a plasmon mode, and as can be observed in Figure 3b, increasing the metal core diameter leads to a redshift in the electric modes and a blueshift in the magnetic until they overlap. Thus in this case we are exclusively observing the stacking of modes of the dielectric shell, where the different electric fields associated with each mode family (in general magnetic modes have a larger

tangential field component than electric modes) lead to different symmetry conditions at the metal boundary, producing a different shift for each mode, which makes this case distinct from the behaviour of materially similar nanoscale structures.

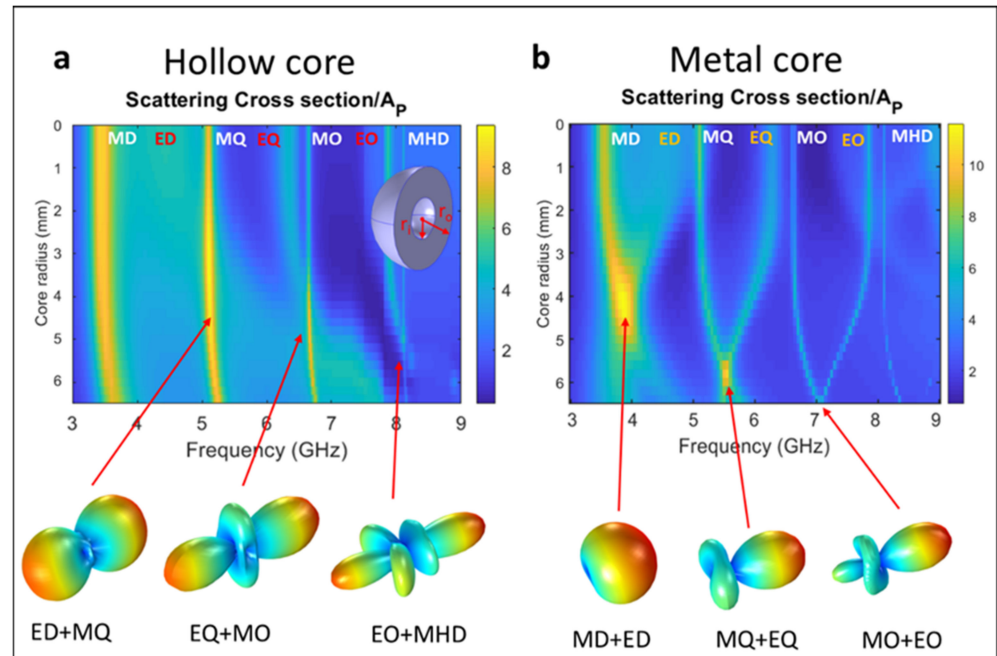


**Figure 3.** Showing the scattering cross section (normalized to the geometric cross section of the particles  $A_p$ ) for a 12.5 mm radius dielectric sphere with a permittivity  $\epsilon = 10.5$  and a loss tangent  $\delta = 0.001$  with varying radius ( $r_i$ ) of (a) air-filled/hollow and (b) metallic core. The inset shows a cross section of the geometry. Each design shows three overlap points between different modes, and the 3D farfield scattering pattern for each combination is shown beneath.

As each mode has a different electric field distribution (Figure 2c), each will be affected differently by the addition of a core, and so different modes will overlap at different frequencies. For the case of the hollow core, it has previously been observed that due to the broad nature of the lower-order modes it is possible to overlap multiple modes simultaneously, leading to multi-band superbackscattering [16], but this is not possible with a metal core due to the fact that all modes are shifting simultaneously. Each mode pairing gives a dramatically different scattering pattern, with higher order pairings giving increasing directionality, as predicted by Liu for core-shell nanoparticles [8]. For the modes investigated here the choice of metal was not seen to be significant. This control over choice of stacked modes has applications wherever one wishes to control the scattering or emission of a dielectric resonator. An interesting course of further study could be to move beyond a spherical core and to try to design dielectric/metallic regions to more closely match the field patterns of a given higher order mode in order to target this mode individually, or at least to a greater degree than all others. We will now discuss two of the most prominent examples of this case at microwave frequencies—controlling the radar cross section (RCS) of an object, and creating directional antennas.

Control of the RCS of small objects is key in fields such as drone detection, autonomous vehicles and cloaking. We carried out an experimental demonstration of the effect of mode stacking to both increase and decrease the RCS of a 12.5 mm radius sphere. Figure 1c,d show the impact of the core shell structure on the first three modes: adding a 4 mm radius metallic core can be shown to reduce the RCS between 3.5–4.5 GHz by approximately a factor of 10, since almost all the scattering is now in the forward direction, as seen in the radiation plots in Figure 3. Reduction in backscatter has numerous applications such as shielding or cloaking small objects and improved performance from metamaterial lenses. For an air core, the mode overlap increases scatter in both the forward and reverse directions

and a 5 mm radius air core can improve the RCS by a factor of 1.5 around the peak at 5.1 GHz. Previous work by the authors has shown that similar enhancements in RCS are possible about multiple peaks simultaneously [16].

The ability to utilize a core-shell structure to achieve mode overlap can also be used to engineer the emission pattern of an antenna. In this case we slice the spheres in half, and place the hemispheres on top of a ground plane, allowing them to be easily fed via a coaxial probe as shown in Figure 4a. Whilst it must be noted that there have been several previous works discussing core-shell hemispherical DRA's [33–37], the focus of these has generally been to broaden the bandwidth of such resonators, and the utility of this system to control the directivity of a DRA has yet to be fully explored.

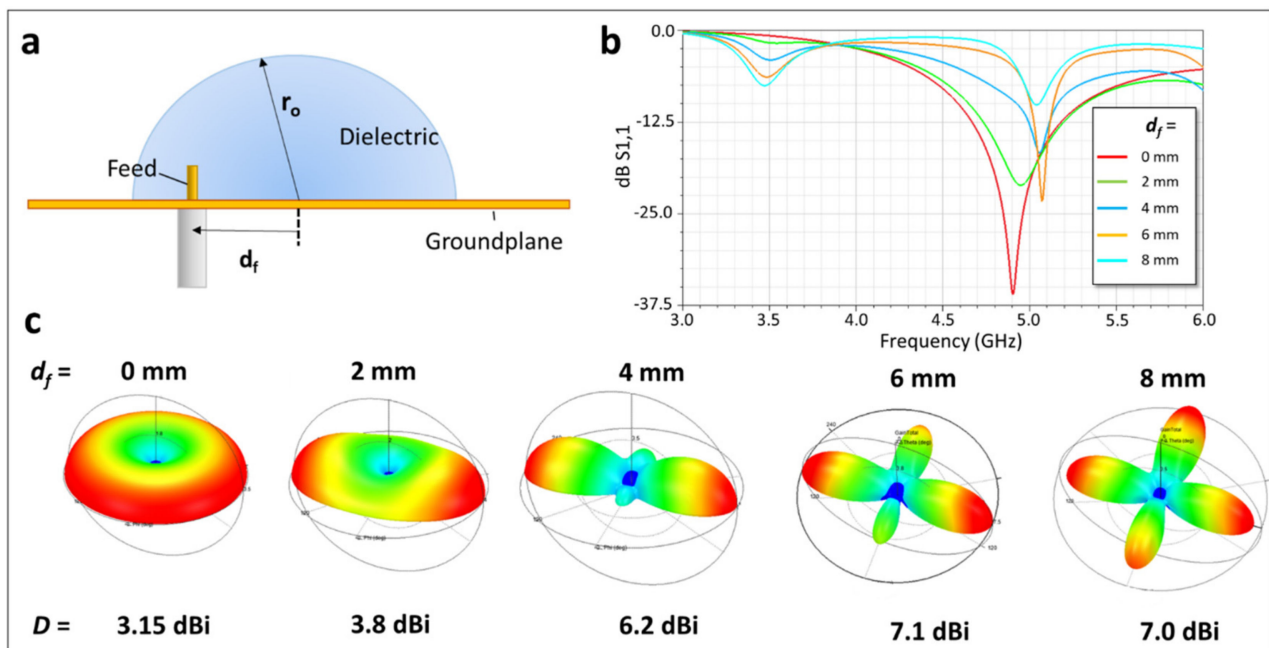


**Figure 4.** (a) A design for a bidirectional hemispherical dielectric resonator antenna based on mode stacking. The hemisphere has a 12.5 mm radius with a permittivity  $\epsilon = 10.5$ . The feed consists of a 4.8 mm long, 1.8 mm diameter feed probe cut from a PTFE-filled coaxial cable with a diameter of 4.1 mm. The groundplane is an infinite PEC. (b) Simulated S11 values from this design as the probe position,  $d_f$  is varied. (c) Directivity plots of all  $d_f$  values simulated, with the maximum directivity, D shown beneath.

Figure 4 shows an Ansys HFSS simulation of a hemispherical antenna design used to achieve bidirectional emission by coupling to the ED and MQ modes simultaneously. This is achieved by simply optimizing  $d_f$ , the position of a 4.8 mm long, 1.3 mm diameter feed probe cut from a coaxial structure corresponding to a standard SMA connector (PTFE-filled coaxial cable with a diameter of 4.1 mm). The properties of the hemispheres are identical to the spheres used previously except that they are now cut in half and modelled on an infinite, perfectly conducting (PEC) ground plane, which creates a symmetry plane for the resonant modes. Excitation is provided from a coaxial waveguide port at the bottom of the probe. It can be observed that when the feed is at the centre of the hemisphere ( $d_f = 0$  mm), there is only a single S11 dip at 4.88 GHz, which corresponds to the excitation of electric dipole, as can be seen from the corresponding emission pattern in Figure 4c. When the feed is moved near the edge of the hemisphere, ( $d_f = 8$  mm), it can be seen that there are two S11 minima at 3.45 and 5.05 GHz. The higher frequency peak can be seen to be quadrupolar in nature from the corresponding emission pattern in Figure 4c, and matches the MQ mode in frequency in Figure 3a, whilst the lower peak corresponds to the MD mode. This is to be expected as the currents in the probe must match the fields one wishes to excite at the location of the feed. Therefore a coaxial probe feed placed at the

centre of the hemisphere, with a ground plane beneath providing a PEC symmetry plane will not match well to the fields of magnetic resonances and will predominantly excite electric modes. Near the edge the reverse is true, and the probe excites mostly magnetic modes. As the feed position is moved across the radius of the hemisphere, changing  $d_f$  can be observed to lead to excitation of both the ED and MQ modes. When ( $d_f = 4$  mm), both modes are excited equally, and the bidirectional emission pattern seen for ED + MQ mode overlap in Figure 3a is again observed. The impedance bandwidth is 0.24 GHz, or 4.75%.

Unidirectional emission can be achieved using a metallic core, as shown in Figure 5. In this instance, a 6 mm long, 1.8 mm diameter feed probe is fixed at  $d_f = 10$  mm and the radius of the metallic core,  $r_i$ , is altered in order to drive the ED and MD modes together both spatially and in frequency. It can be seen that for  $r_i = 5$  mm, which corresponds to the ED + MD overlap in Figure 3b, both the S11 and the directivity are maximised, producing unidirectional emission with an impedance bandwidth of 0.31 GHz or 7.95% and a directivity of 5.4 dBi.

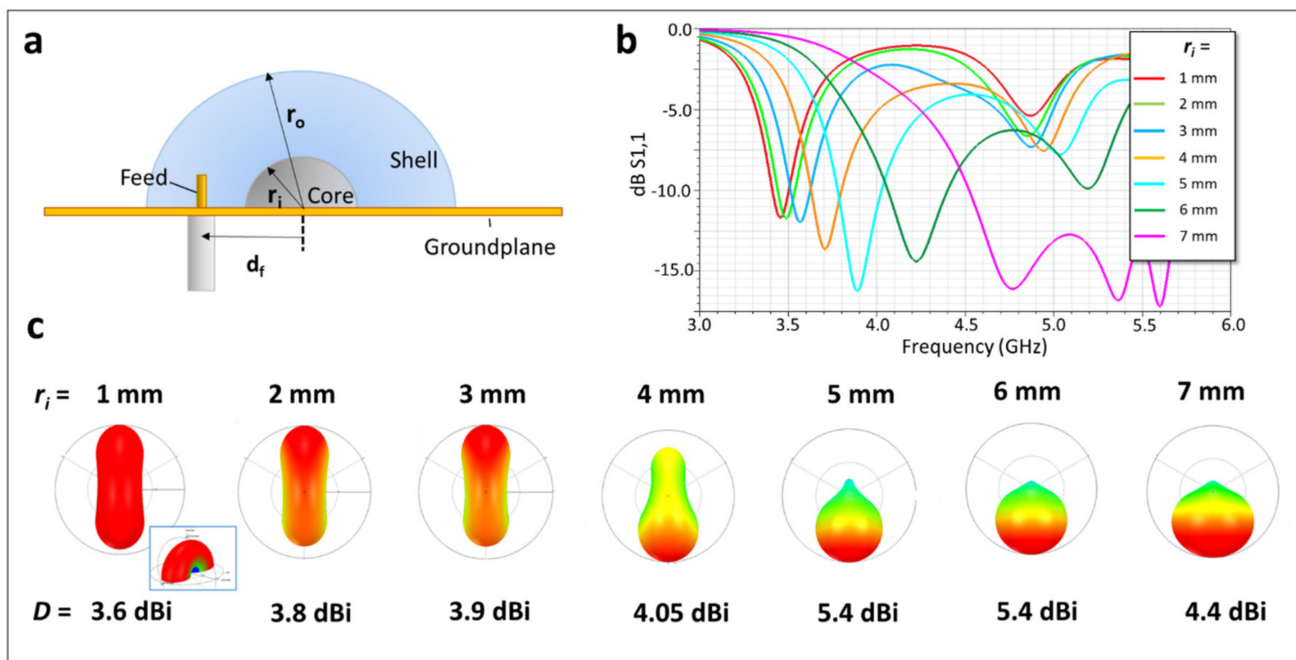


**Figure 5.** (a) A design for a unidirectional hemispherical dielectric resonator antenna based on mode stacking. The hemisphere has a 12.5 mm radius with a permittivity  $\epsilon = 10.5$  and a metallic core with a radius  $r_i$ . The feed consists of a 6 mm long, 1.3 mm diameter feed probe cut from a PTFE-filled coaxial cable with a diameter of 4.1 mm. The groundplane is an infinite PEC. (b) Simulated S11 values from this design as the radius of the metallic core,  $r_i$  is varied. Here the probe position, is fixed at  $d_f = 10$  mm. (c) Directivity plots of all  $r_i$  values simulated, with the maximum directivity,  $D$  shown beneath.

#### 4. Conclusions

In this work we have used the example of a core-shell sphere to demonstrate the versatility of mode stacking in high symmetry dielectric particles, both for maximizing and minimizing the radar cross-section of the particle, and for defining the directivity of a dielectric resonator antenna. We have demonstrated that RCS can be maximised or reduced to almost zero at a given frequency by utilizing an air-filled or metallic core to stack modes whose emissions sum constructively or destructively, respectively, in the backwards direction. We discuss how the same physics can be used to design antennas where multiple modes are driven simultaneously at the same frequency, allowing for bidirectional or unidirectional emission. Combinations of higher order modes will enable even more directional beams and a greater variety of emission patterns.

**Author Contributions:** Conceptualization, A.W.P. and M.M.; methodology, A.W.P. and M.M.; validation, A.W.P. and M.M.; resources, A.W.P., A.P.H. and J.R.S.; writing—original draft preparation, A.W.P.; writing—review and editing, M.M., A.P.H. and J.R.S.; project administration, A.W.P., A.P.H. and J.R.S.; funding acquisition, A.W.P., A.P.H. and J.R.S. All authors have read and agreed to the published version of the manuscript.

**Funding:** This work was funded by the Royal Academy of Engineering, and the Engineering and Physical Sciences Research Council (EPSRC), UK under a Programme Grant (EP/N010493/1) “Synthesizing 3D METAmaterials for RF, microwave and THz applications” (SYMETA).

**Institutional Review Board Statement:** Not applicable.

**Informed Consent Statement:** Not applicable.

**Data Availability Statement:** The data that support the findings of this study are available from the corresponding author upon reasonable request.

**Conflicts of Interest:** The authors declare no conflict of interest. The funders had no role in the design of the study; in the collection, analyses, or interpretation of data; in the writing of the manuscript, or in the decision to publish the results.

## References

1. Qian, C.; Lin, X.; Yang, Y.; Xiong, X.; Wang, H.; Li, E.; Kaminer, I.; Zhang, B.; Chen, H. Experimental Observation of Superscattering. *Phys. Rev. Lett.* **2019**, *122*, 063901. [[CrossRef](#)]
2. Shcherbinin, V.I.; Fesenko, V.I.; Tkachova, T.I.; Tuz, V.R. Superscattering from Subwavelength Corrugated Cylinders. *Phys. Rev. Appl.* **2020**, *13*, 024081. [[CrossRef](#)]
3. Fu, Y.H.; Kuznetsov, A.I.; Miroshnichenko, A.E.; Yu, Y.F.; Luk'yanchuk, B. Directional visible light scattering by silicon nanoparticles. *Nat. Commun.* **2013**, *4*, 1527. [[CrossRef](#)] [[PubMed](#)]
4. Staude, I.; Miroshnichenko, A.E.; Decker, M.; Fofang, N.T.; Liu, S.; Gonzales, E.; Dominguez, J.; Luk, T.S.; Neshev, D.N.; Brener, I.; et al. Tailoring directional scattering through magnetic and electric resonances in subwavelength silicon nanodisks. *ACS Nano* **2013**, *7*, 7824–7832. [[CrossRef](#)]
5. Ruan, Z.; Fan, S. Superscattering of light from subwavelength nanostructures. *Phys. Rev. Lett.* **2010**, *105*, 013901. [[CrossRef](#)] [[PubMed](#)]
6. Geffrin, J.M.; García-Cámara, B.; Gómez-Medina, R.; Albella, P.; Froufe-Pérez, L.S.; Eyraud, C.; Litman, A.; Vaillon, R.; González, F.; Nieto-Vesperinas, M.; et al. Magnetic and electric coherence in forward- and back-scattered electromagnetic waves by a single dielectric subwavelength sphere. *Nat. Commun.* **2012**, *3*, 1171. [[CrossRef](#)]
7. Chen, Z.; Li, Z.; Li, J.; Liu, C.; Lao, C.; Fu, Y.; Liu, C.; Li, Y.; Wang, P.; He, Y. 3D printing of ceramics: A review. *J. Eur. Ceram. Soc.* **2019**, *39*, 661–687. [[CrossRef](#)]
8. Liu, W.; Zhang, J.; Lei, B.; Ma, H.; Xie, W.; Hu, H. Ultra-directional forward scattering by individual core-shell nanoparticles. *Opt. Express* **2014**, *22*, 16178. [[CrossRef](#)] [[PubMed](#)]
9. Qian, C.; Lin, X.; Yang, Y.; Gao, F.; Shen, Y.; Lopez, J.; Kaminer, I.; Zhang, B.; Li, E.; Soljačić, M.; et al. Multifrequency Superscattering from Subwavelength Hyperbolic Structures. *ACS Photonics* **2018**, *5*, 1506–1511. [[CrossRef](#)]
10. Liu, W.; Lei, B.; Shi, J.; Hu, H. Unidirectional superscattering by multilayered cavities of effective radial anisotropy. *Sci. Rep.* **2016**, *6*, 34775. [[CrossRef](#)] [[PubMed](#)]
11. Jin, P.; Ziolkowski, R.W. Metamaterial-inspired, electrically small Huygens sources. *IEEE Antennas Wirel. Propag. Lett.* **2010**, *9*, 501–505. [[CrossRef](#)]
12. Gómez-Medina, R.; García-Cámara, B.; Suárez-Lacalle, I.; González, F.; Moreno, F.; Juan, M.N.-V.; Sáenz, J.; Nieto-Vesperinas, M.; Sáenz, J.J. Electric and magnetic dipolar response of germanium nanospheres: Interference effects, scattering anisotropy, and optical forces. *J. Nanophotonics* **2011**, *5*, 053512. [[CrossRef](#)]
13. Liu, W.; Miroshnichenko, A.E.; Neshev, D.N.; Kivshar, Y.S. Polarization-independent Fano resonances in arrays of core-shell nanoparticles. *Phys. Rev. B* **2012**, *86*, 081407. [[CrossRef](#)]
14. Person, S.; Jain, M.; Lapin, Z.; Sáenz, J.J.; Wicks, G.; Novotny, L. Demonstration of zero optical backscattering from single nanoparticles. *Nano Lett.* **2013**, *13*, 1806–1809. [[CrossRef](#)]
15. Abdelrahman, M.I.; Saleh, H.; Fernandez-Corbaton, I.; Gralak, B.; Geffrin, J.M.; Rockstuhl, C. Experimental demonstration of spectrally broadband Huygens sources using low-index spheres. *APL Photonics* **2019**, *4*, 020802. [[CrossRef](#)]
16. Powell, A.W.; Hibbins, A.P.; Sambles, J.R. Multiband superbackscattering via mode superposition in a single dielectric particle. *Appl. Phys. Lett.* **2021**, *118*, 251107. [[CrossRef](#)]
17. Atwater, H.A.; Polman, A. Plasmonics for improved photovoltaic devices. *Nat. Mater.* **2010**, *9*, 205–213. [[CrossRef](#)] [[PubMed](#)]
18. Powell, A.W.; Wincott, M.B.; Watt, A.A.R.; Assender, H.E.; Smith, J.M. Controlling the optical scattering of plasmonic nanoparticles using a thin dielectric layer. *J. Appl. Phys.* **2013**, *113*, 184311. [[CrossRef](#)]

19. Powell, A.W.; Ware, J.; Beadle, J.G.; Cheadle, D.; Loh, T.H.; Hibbins, A.P.; Roy Sambles, J. Strong, omnidirectional radar backscatter from subwavelength, 3D printed metacubes. *IET Microwaves Antennas Propag.* **2020**, *14*, 1862–1868. [[CrossRef](#)]
20. Tribelsky, M.I.; Luk'yanchuk, B.S. Anomalous light scattering by small particles. *Phys. Rev. Lett.* **2006**, *97*, 263902. [[CrossRef](#)] [[PubMed](#)]
21. Elancheliyan, R.; Dezert, R.; Castano, S.; Bentaleb, A.; Nativ-Roth, E.; Regev, O.; Barois, P.; Baron, A.; Mondain-Monval, O.; Ponsinet, V. Tailored self-assembled nanocolloidal Huygens scatterers in the visible. *Nanoscale* **2020**, *12*, 24177–24187. [[CrossRef](#)] [[PubMed](#)]
22. Liberal, I.; Ederra, I.; Gonzalo, R.; Ziolkowski, R.W. Superbackscattering from single dielectric particles. *J. Opt.* **2015**, *17*, 072001. [[CrossRef](#)]
23. Naraghi, R.R.; Sukhov, S.; Dogariu, A. Directional control of scattering by all-dielectric core-shell spheres. *Opt. Lett.* **2015**, *40*, 585. [[CrossRef](#)] [[PubMed](#)]
24. Boyuan, M.; Pan, J.; Huang, S.; Yang, D.; Guo, Y.X. Unidirectional Dielectric Resonator Antennas Employing Electric and Magnetic Dipole Moments. *IEEE Trans. Antennas Propag.* **2021**, *69*, 6918–6923. [[CrossRef](#)]
25. Guo, L.; Leung, K.W.; Yang, N. Wide-Beamwidth Unilateral Dielectric Resonator Antenna Using Higher-Order Mode. *IEEE Antennas Wirel. Propag. Lett.* **2019**, *18*, 93–97. [[CrossRef](#)]
26. Ma, B.; Pan, J.; Huang, S.; Yang, D.; Guo, Y.X. Wideband Endfire Dielectric Resonator Antenna Employing Fundamental and Higher-Order Magnetolectric Resonances. *IEEE Antennas Wirel. Propag. Lett.* **2021**, *20*, 2524–2528. [[CrossRef](#)]
27. Krasnok, A.E.; Miroshnichenko, A.E.; Belov, P.A.; Kivshar, Y.S. Huygens optical elements and Yagi-Uda nanoantennas based on dielectric nanoparticles. *JETP Lett.* **2011**, *94*, 593–598. [[CrossRef](#)]
28. Krasnok, A.E.; Simovski, C.R.; Belov, P.A.; Kivshar, Y.S. Superdirective dielectric nanoantennas. *Nanoscale* **2014**, *6*, 7354–7361. [[CrossRef](#)]
29. Hancu, I.M.; Curto, A.G.; Castro-López, M.; Kuttge, M.; Van Hulst, N.F. Multipolar Interference for Directed Light Emission. *Nano Lett.* **2013**, *14*, 166–171. [[CrossRef](#)] [[PubMed](#)]
30. Jacobsen, R.E.; Lavrinenko, A.V.; Arslanagic, S. A Water-Based Huygens Dielectric Resonator Antenna. *IEEE Open J. Antennas Propag.* **2020**, *1*, 493–499. [[CrossRef](#)]
31. Premix. Available online: <https://www.premixgroup.com/> (accessed on 10 November 2021).
32. Liu, W.; Kivshar, Y.S. Generalized Kerker effects in nanophotonics and meta-optics [Invited]. *Opt. Express* **2018**, *26*, 13085. [[CrossRef](#)] [[PubMed](#)]
33. Leung, K.W.; Lai, K.Y.A.; Luk, K.M.; Lin, D. Theory and Experiment of a Coaxial Probe Fed Hemispherical Dielectric Resonator Antenna. *IEEE Trans. Antennas Propag.* **1993**, *41*, 1390–1398. [[CrossRef](#)]
34. Leung, K.W.; So, K.K. Theory and experiment of the wideband two-layer hemispherical dielectric resonator antenna. *IEEE Trans. Antennas Propag.* **2009**, *57*, 1280–1284. [[CrossRef](#)]
35. Leung, K.W.; Luk, K.M.; Lai, K.Y.A.; Lin, D. Theory and experiment of an aperture-coupled hemispherical dielectric resonator antenna. *IEEE Trans. Antennas Propag.* **1995**, *43*, 1192–1198. [[CrossRef](#)]
36. Wong, K.L.; Chen, N.C.; Chen, H.T. Analysis of a Hemispherical Dielectric Resonator Antenna with an Airgap. *IEEE Microw. Guid. Wave Lett.* **1993**, *3*, 355–357. [[CrossRef](#)]
37. Leung, K.W. Complex resonance and radiation of hemispherical dielectric-resonator antenna with a concentric conductor. *IEEE Trans. Microw. Theory Tech.* **2001**, *49*, 524–531. [[CrossRef](#)]